# Dalton Transactions

Accepted Manuscript

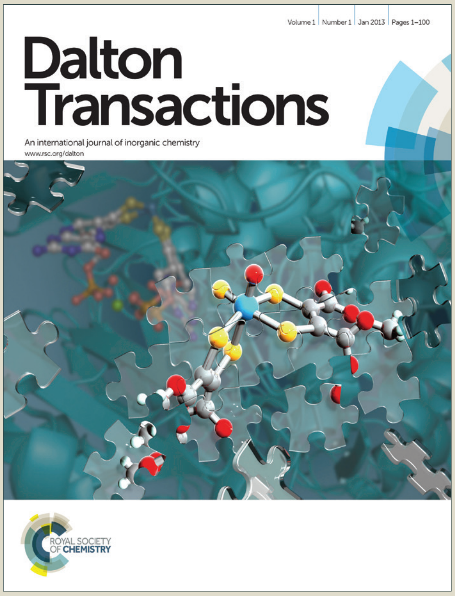

ROYAL SOCIETY OF CHEMISTRY

www.rsc.org/dalton

# TABLE OF CONTENTS ENTRY

## Four New Trinuclear $\{Cu_3(\mu_3\text{-}OH)(oximate)_3\}^{2+}$ Clusters: Crystal Structure and Magnetic Behaviour.†

**Saskia Speed, Mercè Font-Bardia, M. Salah El Fallah and Ramon Vicente**

Four new triangular copper(II) complexes with the fragment $\{Cu_3(\mu_3\text{-}OH)(oximate)_3\}^{2+}$ are reported. They exhibit strong antiferromagnetic coupling and antisymmetric exchange interaction.

## Artwork

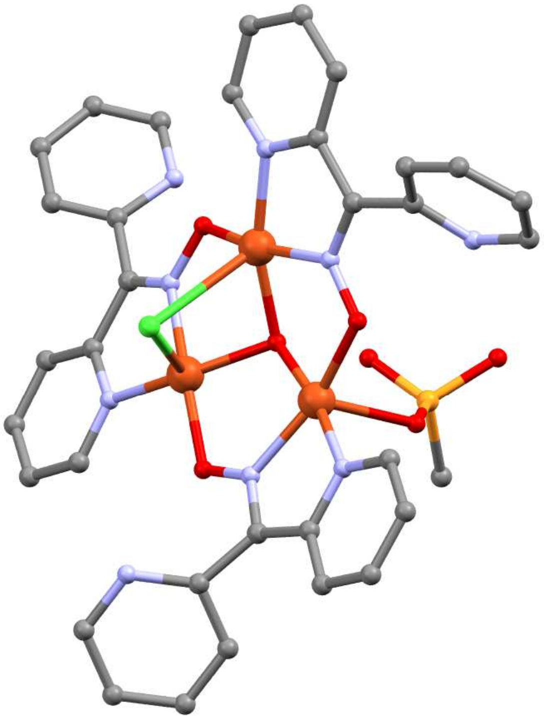

# Four New Trinuclear $\{Cu_3(\mu_3\text{-}OH)(oximate)_3\}^{2+}$ Clusters: Crystal Structure and Magnetic Behaviour.†

**Saskia Speed,[a]* Mercè Font-Bardia,[b] M. Salah El Fallah[a] and Ramon Vicente[a]***

Four new triangular copper(II) complexes with the fragment $\{Cu_3(\mu_3\text{-}OH)(oximate)_3\}^{2+}$ and formulae $[Cu_3(\mu_3\text{-}OH)(\mu\text{-}Cl)(Py_2CNO)_3(^tBuPO_3H)]\cdot 4H_2O$ **(1)**, $[Cu_3(\mu_3\text{-}OH)(\mu\text{-}Br)(Py_2CNO)_3(^tBuPO_3H)]\cdot 3.5H_2O$ **(2)**, $[Cu_3(\mu_3\text{-}OH)(\mu\text{-}Br)(PhPyCNO)_3(^tBuPO_3H)(MeOH)]\cdot 1.5MeOH$ **(3)**, $[Cu_3(\mu_3\text{-}OH)Cl_2(PhPyCNO)_3]\cdot 0.5H_2O$ **(4)**, ($Py_2CNO$ = di(2-pyridyl)ketoximate, PhPyCNO = phenyl(2-pyridyl)ketoximate, $^tBuPO_3H_2$ = *tert*-butylphosphonic acid) are reported. The magnetic properties of compounds **1-4** have been studied. The compounds were found to exhibit strong antiferromagnetic coupling and antisymmetric exchange interaction.

## Introduction

The reaction of oximate ligands with paramagnetic 3d metal ions can generate polynuclear complexes with interesting magnetic properties, including single-molecule magnet behaviour.[1-7] Among the polynuclear oximate compounds, a great number of isolated triangles with the $\{Cu_3(\mu_3\text{-}OR)(oximate)_3\}^{n+}$ core have been well characterized.[8-21] The magnetic response of these small molecules can be useful for determining the factors that influence the magnetic coupling and for studying the spin frustration phenomenon by testing the magnetic exchange models.[22] The $\{Cu_3(\mu_3\text{-}OR)(oximate)_3\}^{n+}$ core is also in the basis of discrete hexanuclear copper(II) cages with the $[Cu_3O\ldots H\ldots OCu_3]$ motif.[23-28]

On the other hand, the phosphonate ligands can also generate polynuclear complexes with interesting magnetic properties, including single-molecule magnet behaviour.[29] A possibility to explore can be to combine in the same synthesis oximate and phosphonate ligands with copper(II) salts to try to obtain new polynuclear Cu(II) complexes with new topologies. By reaction between copper(II) methoxide, oximate ligands, *tert*-butylphosphonic acid and halides we have obtained

---

[a] Departament de Química Inorgànica, Universitat de Barcelona, Martí i Franquès 1-11, 08028 Barcelona, Spain. E-mail: ramon.vicente@qi.ub.es (RV), saskia.speed@qi.ub.es (SS).

[b] Departament de Cristal·lografia i Minerologia, Universitat de Barcelona, Martí i Franquès s/n, 08028 Barcelona, Spain.

[†] Electronic supplementary information (ESI) available. CCDC reference numbers 1014421-1014424. For ESI and crystallographic data in CIF or other electronic format see DOI:******

four new triangular copper(II) compounds with the fragment $\{Cu_3(\mu\text{-}OH)(oximate)_3\}^{2+}$ and formulae $[Cu_3(\mu_3\text{-}OH)(\mu\text{-}Cl)(Py_2CNO)_3({}^tBuPO_3H)]\cdot 4H_2O$ **(1)**, $[Cu_3(\mu_3\text{-}OH)(\mu\text{-}l)(Py_2CNO)_3({}^tBuPO_3H)]\cdot 3.5H_2O$ **(2)**, $[Cu_3(\mu_3\text{-}OH)(\mu\text{-}Br)(PhPyCNO)_3({}^tBuPO_3H)(MeOH)]\cdot 1.5MeOH$ **(3)**, $[Cu_3(\mu_3\text{-}OH)Cl_2(PhPyCNO)_3]\cdot 0.5H_2O$ **(4),** ($Py_2CNO$ = di(2-pyridyl)ketoximate, PhPyCNO = phenyl(2-pyridyl)ketoximate, ${}^tBuPO_3H_2$ = *tert*-butylphosphonic acid). In three of the new trinuclear compounds (**1-3**) there is a ${}^tBuPO_3H^-$ ligand axially coordinated to one of the copper atoms and one $Cl^-$ or $Br^-$ ligand bridging the other two copper atoms. In the fourth complex the hydrogenphosphonate is not present and the $Cl^-$ ligand doesn't bridge two copper atoms but instead there are two terminal $Cl^-$ ligands. Compounds **1-3** show a known topology in copper oximato compounds: triangular systems with oximato bridging ligands containing a central $\mu_3$-hydroxo and two potentially chelating anions coordinated to the axial coordination sites of the copper atoms on opposite sides of the triangle faces, one of them bridging two copper atoms and the other as terminal. These anions are usually carboxylate ligands.[14,17,20,21] In the case of compounds **1-3** the terminal ligand is a hydrogenphosphonate that is stabilized by hydrogen bond with the central $\mu_3$-hydroxo ligand and one $Cl^-$ or $Br^-$ ligand bridging the other two copper atoms on opposite sides. The other usual topology found in copper oximato chemistry are dinuclear compounds with very strong antiferromagnetic coupling (-J around 500 $cm^{-1}$).[17,30]

From the magnetic point of view, in a copper(II) equilateral triangle (Scheme 1), taking into account the isotropic Hamiltonian $\hat{H} = -\sum_{i,j} J_{i,j}\hat{S}_i\hat{S}_j$, the derived equation for the magnetic susceptibility in function of the temperature is:

$$\chi_M = \frac{Ng^2\beta^2}{4kT}\frac{1+5\exp(x)}{1+\exp(x)} \qquad (1)$$

where $x = 3J/2kT$. By using equation (1) to fit the experimental magnetic susceptibility values measured in triangular copper(II) complexes, it is usually found an obvious discrepancy mainly in the low-temperature magnetic data where the $\chi_M T$ value is smaller than that for one unpaired electron. This discrepancy arises mainly from the non consideration in equation (1), derived from the isotropic Hamiltonian, of the intramolecular antisymmetric exchange.[22]

Recently, F. Lloret and co-workers have published a new equation which includes the intramolecular antisymmetric exchange and the Zeeman interactions.[22] This equation has been used to fit the experimental magnetic data of the new compounds **1-4**.

Insert Scheme 1 close to here

## Results and discussion

### Synthesis

Previous attempts to prepare copper(II)/tert-butylphosphonate/oximate compounds without halide salts were unsuccessful. The structural determination of **1** in a few crystals formed in an attempt without halide salts but due to the existence of a little quantity of chloride impurities in the starting copper methoxide salt decided us to attempt the synthesis by adding halide salts to the reaction mixture. The starting copper salt was copper(II) methoxide to avoid another anion to be present in the reaction and also to generate basic medium. The solvent was methanol. The stoichiometric equations for reactions **1-4** were: 1 Cu(II) methoxide + 1 oxime + 1 *tert*-butylphosphonic acid + 0.23 NaCl. Taking into account the formulae of compounds **1-3**, the toichiometric coefficient of NaCl was minor to the necessary (0.33) to favour the *tert*-butylphosphonate as a ligand in the final compound.

### Description of the structures of compounds 1 and 2.

The structures of compounds **1** and **2** are very similar and differ mainly in the bridging halide, chlorine in **1** and bromine in **2**, and in the number of lattice water molecules. The structural parameters of complex **2** will be next to the corresponding ones of complex **1**.

The structures of compounds **1** and **2** consist of triangular [Cu$_3$($\mu_3$-OH)($\mu$-X)(Py$_2$CNO)$_3$($^t$BuPO$_3$H)] units, X = Cl (**1**), Br (**2**), (Figures 1 and 3) and lattice water molecules. Selected bond distances and angles are listed in Tables 1 and 2. The geometry around each of the copper(II) ions in the trimeric units is best described as a distorted square pyramid ($\tau$ = 0.046/0.053 for Cu1, 0.165/0.181 for Cu2 and 0.187/0.182 for Cu3, $\tau$ = Addison parameter. $\tau$ = 0 for an ideal square base pyramid and□ $\tau$ = 1 for an ideal trigonal bipyramid).[31] Two of the copper ions (Cu1 and Cu3) have a NNOOX coordination environment, whereas the third copper ion (Cu2) has a NNOOO coordination environment. The trimeric skeleton is created by the oximato nitrogen atoms of one Py$_2$CNO$^-$ ligand and the oxime oxygen atom of the adjacent Py$_2$CNO$^-$ligand, while the O atom of the $\mu_3$-OH$^-$ ligand (O1) completes the square-planar bases of the three metal atoms, with Cu1-O1, Cu2-O1, and Cu3-O1 bond distances of 1.947(4)/1.939(3), 1.931(3)/1.928(3), and 1.947(4)/1.944(3) Å, respectively. The bidentate chloride ligand bridges Cu1 and Cu3, with Cu1-X1 and Cu3-X1 distances of 2.633(6)/2.855(1) and 2.684(5)/2.740(1) Å, respectively, while the oxygen of the monodentate $^t$BuPO$_3$H$^-$ ligand occupies the apical position of the Jahn-Teller-elongated square pyramid of Cu2, with a Cu2-O5 distance of 2.293(4)/2.276(4) Å.

The oximate bridges, Cu-N-O-Cu', deviate slightly from planarity, with torsion angles of -3.1(4)º/-1.8(4)º (Cu1-N2-O2-Cu2), -17.7(6)º/-18.8(5)º (Cu2-N5-O3-Cu3), and -4.8(4)º/-4.9(4)º (Cu3-N8-O4-Cu1). The [Cu$_3$] unit is strictly an scalene triangle, but can be considered as an isosceles triangle with Cu1...Cu2, Cu1...Cu3, and Cu2...Cu3 distances of 3.240/3.232, 3.042/3.042, and 3.229/3.232 Å, respectively. The oxygen atom of the hydroxo ligand, which is trapped in the metallacrown ring, lies at 0.638/0.625 Å out of the plane defined by the copper atoms.

There are intra- and intermolecular H-bonds. The capping $\mu_3$-OH hydrogen is engaged in a H-bond with an oxygen of the *tert*-butylphosphonate ligand [O1···O6 2.557(5)/2.546(4) Å; O1-H1A···O6 171(3)/167(3)º], whereas the other oxygen atom of the *tert*-butylphosphonate ligand makes intermolecular H-bonds with the *tert*-butylphosphonate ligand [O7···O6' 2.600(4)/2.590(4) Å; O7-H7A···O6' 177(6)/155.00º; ': -x,-y,1-z//1-x,-y,1-z] of other trinuclear unit, forming dimers of trimers not further connected (Figures 2 and 4).

Insert Figures 1-4, Table 1 and 2 close to here

### Description of the structure of compound 3.

The structure of **3** consists of a triangular [Cu$_3$($\mu_3$-OH)($\mu$-Br)(PhPyCNO)$_3$($^t$BuPO$_3$H)(MeOH)] unit (Figure 5) and one and a half lattice methanol molecules. Selected bond distances and angles are listed in Table 3. The geometry around two of the copper(II) ions in the trimeric unit is best described as a distorted square pyramid ($\tau = 0.159$ for Cu2 and 0.101 for Cu3).[31] Cu2 has a NNOOO coordination environment, while Cu3 has a NNOOBr coordination environment. The third copper atom (Cu1) is hexacoordinated with a NNOOOBr coordination environment. The trimeric skeleton is created by the oximato nitrogen atoms of one PhPyCNO$^-$ ligand and the oxime oxygen atom of the adjacent PhPyCNO$^-$ligand, whereas the O atom of the $\mu_3$-OH$^-$ ligand

(O1) completes the square-planar bases of the three metal atoms, with Cu1-O1, Cu2-O1, and Cu3-O1 bond distances of 1.933(2), 1.948(2), and 1.967(3) Å, respectively. The bidentate bromide ligand bridges Cu1 and Cu3, with Cu1-Br1 and Cu3-Br1 distances of 3.123(1) and 2.726(1) Å, respectively, whereas the oxygen of the monodentate $^{t}BuPO_3H^-$ ligand occupies the apical position of the Jahn-Teller-elongated square pyramid of Cu2, with a Cu2-O5 distance of 2.316(3) Å. The sixth coordination position of Cu1 is occupied by an oxygen atom of a methanol ligand with a Cu1-O8 distance of 2.537(5) Å.

The oximate bridges, Cu-O-N-Cu’, deviate slightly from planarity, with torsion angles of -9.8(4)º (Cu1-O4-N6-Cu3), -11.0(4)º (Cu2-O2-N2-Cu1), and -18.0(4)º (Cu3-O3-N4-Cu2). The [$Cu_3$] unit, as in compound **1**, can be considered as an isosceles triangle with Cu1...Cu2, Cu1...Cu3, and Cu2...Cu3 distances of 3.218, 3.104, and 3.190 Å, respectively. The oxygen atom of the hydroxo ligand, which is trapped in the metallacrown ring, lies at 0.665 Å out of the plane defined by the copper atoms.

There are intra- and intermolecular H-bonds. The capping $\mu_3$-OH hydrogen is engaged in a H-bond with an oxygen of the *tert*-butylphosphonate ligand [O1···O7 2.642(4) Å; O1-H1A···O7 157(4)º], whereas the other oxygen atom of the *tert*-butylphosphonate ligand makes intermolecular H-bonds with another *tert*-butylphosphonate ligand [O6···O5’ 2.609(4) Å; O6-H6A···O5’ 172(6)º; ‘: -x,1-y,-z] forming dimers of trimers not further connected (Figure 6). There is also a hydrogen bond involving the terminal methanol and the *tert*-butylphosphonate ligands [O8...O7 2.731(5) Å; O8-H8A...O7 174(7)º] (Figure 6).

Insert Figures 5 and 6, Table 3 close to here

## Description of the structure of compound 4.

The structure of **4** consists of a triangular [$Cu_3(\mu_3\text{-}OH)Cl_2(PhPyCNO)_3$] unit (Figure 7) and one half lattice water molecule. Selected bond distances and angles are listed in Table 4. The geometry around two of the copper(II) ions in the trimeric unit is best described as a distorted square pyramid ($\tau$ = 0.006 for Cu1, and 0.223 for Cu3)[31] with a NNOOCl coordination environment, while the third copper ion (Cu2) has a NNOO coordination environment. The trimeric skeleton is created by the oximato nitrogen atoms of one $PhPyCNO^-$ ligand and the oxime oxygen atom of the adjacent $PhPyCNO^-$ligand, whereas the O atom of the $\mu_3$-$OH^-$ ligand

(O1) completes the square-planar bases of the three metal atoms, with Cu1-O1, Cu2-O1, and Cu3-O1 bond distances of 1.986(2), 1.944(2), and 1.989(3) Å, respectively. The apical position of Cu1 and Cu3 are occupied by two monodentate chloride ligands with Cu1-Cl1 and Cu3-Cl2 distances of 2.508(2) and 2.600(2) Å, respectively.

The oximate bridges, Cu-O-N-Cu', deviate slightly from planarity, with torsion angles of 3.5(3)º (Cu1-O4-N6-Cu3), 32.7(3)º (Cu2-O2-N2-Cu1), and 17.7(3)º (Cu3-O3-N4-Cu2). The [$Cu_3$] unit can also be considered as an isosceles triangle with Cu1...Cu2, Cu1...Cu3, and Cu2...Cu3 distances of 3.207, 3.189, and 3.106 Å, respectively. The oxygen atom of the hydroxo ligand, which is trapped in the metallacrown ring, lies at 0.739 Å out of the plane defined by the copper atoms.

There is an intermolecular H-bond. The capping $\mu_3$-OH hydrogen is engaged in a H-bond with a chloride ligand [O1···Cl1 3.045(3) Å; O1-H1A···Cl1 170(4)º; ': -x,y,1/2-z] of other trinuclear unit, forming dimers of trimers not further connected (Figure 8).

Insert Figures 7 and 8, Table 4 close to here

## Magnetic properties

The magnetic properties of compounds **1-4** in the form of $\chi_M T$ vs. T plot are shown in Figure 9. At room temperature, the $\chi_M T$ values are in the range of 0.46-0.53 $cm^3 \cdot K \cdot mol^{-1}$ per trinuclear unit. These values are appreciably lower than those expected for three noninteracting S = ½ ions ($\chi_M T$ = 1.125 $cm^3 \cdot K \cdot mol^{-1}$, g = 2.0), suggesting very strong antiferromagnetic coupling. When the samples are cooled, $\chi_M T$ decreases continuously reaching values in the range of 0.26-0.34 $cm^3 \cdot K \cdot mol^{-1}$ at 2 K. These $\chi_M T$ vs. T curves clearly indicate strong intratrimer antiferromagnetic coupling. As first approximation, it is often assumed that the three metal ions are structurally equivalent and the isotropic spin Hamiltonian $\hat{H} = -\sum_{i,j} J_{i,j} \hat{S}_i \hat{S}_j$ can be used to describe the magnetic interactions through equation (1). An attempt to use this approach, however, failed to reproduce the low-temperature decrease in the $\chi_M T$ vs. T plot for compounds **1-4**. Different *J* and *g* values for the different magnetic centres do not improve the fit and lead to overparametrization.

The magnetic behaviour of the {$Cu_3(\mu_3$-OH)} core has been extensively studied and S. Ferrer et al. have published a comprehensive review of the field.[22] Taking into account this last paper, a new approach assuming the contribution of the antisymmetric exchange was considered. To fit the experimental data for compounds **1-4**, we used the following Hamiltonian:

$$\hat{H} = \hat{H}_{iso} + \hat{H}_{ASE} + \hat{H}_{Zeem}$$

where $H_{iso}$ is a Hamiltonian for isotropic exchange for an isosceles triangle with parameters $J = J_{12} = J_{23}$ and $j = J_{13}$; $H_{ASE}$ is an axial Hamiltonian for the antisymmetric exchange with $G_Z$ parallel to the $C_3$ axis and $G_\perp = 0$; $H_{Zeem}$ is an axial Hamiltonian for the Zeeman interaction with $g_{\parallel} = g_{1z} = g_{2z} = g_{3z}$ and $g_\perp = g_{1x} = g_{2x} = g_{3x} = g_{1y} = g_{2y} = g_{3y}$. The exact analytical expression for the molar magnetic susceptibility in function of the temperature can be found in reference 22.

The best-fit parameters found in the fitting of the magnetic susceptibility experimental data for compounds **1-4** are listed in Table 5 and the theoretical curves calculated from these parameters are depicted as solid lines in Figure 9.

Insert Figure 9 and Table 5 close to here

## Magnetostructural Correlations.

The more relevant structural parameters (bond lengths and angles) together with the exchange parameters for complexes **1-4** are listed in Table 6. These parameters are depicted in Scheme 2. The Cu-N,O and Cu-OH bond lengths ($d_{Cu\text{-}ox}$ and $d_{Cu\text{-}OH}$, respectively) are the mean values for each compound. The β angle is defined by the average of the two most similar Cu-O-Cu angles within the triangle, whereas the γ angle refers to the most different one and the $\alpha_{av}$ angle is defined as $(2\beta + \gamma)/3$. Finally, the values of the exchange parameters are as follows: $J = J_{12} = J_{13}$, $j = J_{23}$, and $J_{av} = (2J + j)/3$.

The magnetic interaction between two copper(II) ions within the triangle is mediated by both the diatomic N,O-(oxime) and the monatomic O-(hydroxo) bridges. The structural parameters associated with the oxime bridge are comparable in the four compounds. The hydroxo bridge also presents similar Cu-O distances (1.93−1.99 Å) in **1-4** and no relation is appreciated between this small variation and the values of the exchange coupling parameters. The magnetostructural correlation involves mainly the Cu-O-Cu bridgehead angle. In this respect, as observed in Table 6, the $J_{av}$, $J$, and $j$ parameters depend on the $\alpha_{av}$, β, and γ angles, respectively: the larger the angle, the larger the magnetic coupling. So, given that $\beta > \gamma$, then $|J| > |j|$, except for compound **4**, for which $\gamma > \beta$ and $|j| > |J|$. It is worth noting that the Cu-O-Cu angle is directly related with the out-of-plane shift of the hydroxo bridge from the plane defined by the three copper atoms: the larger the shift, the smaller the angles. In fact, for similar compounds, it has been suggested that the more flattened the $Cu_3O(H)$ bridge (i.e., Cu-O-Cu angles closer to 120°), the stronger the magnetic interaction.[18] A plot of the Cu-O-Cu angle *vs.* the exchange coupling constant is shown in Figure 10. The best linear fit is expressed by equation (2), where $J$ is given in $cm^{-1}$.

$$J = -19.08\theta + 1656 \qquad (2)$$

The equation (2) is valid for compounds with the $\{Cu_3(\mu_3\text{-}OH)(oximate)_3\}^{2+}$ fragment. Although the number of examples presented herein is hardly sufficient to establish a final accurate correlation, it may be concluded that the Cu-O-Cu bridgehead angle is one of the main factors governing the nature and magnitude of the magnetic coupling in the $\{Cu_3(\mu_3\text{-}OH)(oximate)_3\}^{2+}$ triangular tricopper(II) complexes.

Insert Figure 10, Table 6 and Scheme 2 close to here

## Experimental

### Materials and physical measurements

All reagents, metal salt and ligands were used as obtained from Aldrich. Infrared spectra (4000-400 $cm^{-1}$) were recorded from KBr pellets on a Perkin-Elmer 380-B spectrophotometer. Magnetic susceptibility measurements under magnetic fields of 0.3 T in the temperature range 2-300 K and magnetization measurements in the field range of 0-5 T were performed with a Quantum Design MPMS-XL SQUID magnetometer at the Magnetic Measurements Unit of the University of Barcelona. All measurements were performed on polycrystalline samples. Pascal's constants were used to estimate the diamagnetic corrections, which were subtracted from the experimental susceptibilities to give the corrected molar magnetic susceptibilities.

### Synthesis of $[Cu_3(\mu_3\text{-}OH)(\mu\text{-}Cl)(Py_2CNO)_3(C_4H_9PO_3H)]\cdot 4H_2O$ (1)

All reagents, metal salt and ligands were used as obtained from Aldrich.

To a solution of Cu(II) methoxide (0.201 g, 1.6 mmol) in methanol was added di-2-pyridyl ketone oxime ($Py_2CNOH$, 0.319 g, 1.6 mmol), *tert*-butylphosphonic acid ($^tBuPO_3H_2$, 0.221 g, 1.6 mmol) and NaCl (0.021 g, 0.36 mmol). After a few days of slow evaporation compound **1** was obtained as blue prism crystals. Anal.: Found: C, 42.6; H, 4.0; N, 12.0. Calcd. for

$C_{37}H_{43}ClCu_3N_9O_{11}P$: C, 42.5; H, 4.1; N, 12.0%. Selected IR data (KBr)/cm$^{-1}$: 3423 (br), 2925 (m), 2854 (m), 1598 (s), 1529 (m), 1464 (s), 1437 (m), 1127 (vs), 1106 (m), 1054 (m), 898 (m).

**Synthesis of [$Cu_3(\mu_3$-OH)($\mu$-Br)($Py_2CNO)_3(C_4H_9PO_3H)]\cdot 3.5H_2O$ (2)**

To a solution of Cu(II) methoxide (0.201 g, 1.6 mmol) in methanol was added di-2-pyridyl ketone oxime ($Py_2CNOH$, 0.319 g, 1.6 mmol), *tert*-butylphosphonic acid ($^tBuPO_3H_2$, 0.221 g, 1.6 mmol) and KBr (0.043 g, 0.36 mmol). After a few days of slow evaporation compound **1** was obtained as blue prism crystals. Anal.: Found: C, 41.0; H, 3.7; N, 12.0. Calcd. for $C_{37}H_{43}BrCu_3N_9O_{11}P$: C, 40.7; H, 4.0; N, 11.6%. Selected IR data (KBr)/cm$^{-1}$: 3424 (br), 2960 (m), 2856 (m), 1598 (m), 1529 (m), 1464 (s), 1437 (m), 1127 (vs), 1105 (m), 1054 (m), 898 (m).

**Synthesis of [$Cu_3(\mu_3$-OH)($\mu$-Br)($PhPyCNO)_3(C_4H_9PO_3H)]\cdot 1.5MeOH$ (3)**

To a solution of Cu(II) methoxide (0.201 g, 1.6 mmol) in methanol was added phenyl 2-pyridyl ketoxime (PhPyCNOH, 0.317 g, 1.6 mmol), *tert*-butylphosphonic acid ($^tBuPO_3H_2$, 0.221 g, 1.6 mmol) and KBr (0.043 g, 0.36 mmol). After a few days of slow evaporation compound **1** was obtained as blue prism crystals. Anal.: Found: C, 46.0; H, 4.1; N, 8.0. Calcd. for $C_{41}H_{42}BrCu_3N_6O_8P$: C, 47.0; H, 4.0; N, 8.0 %. Selected IR data (KBr)/cm$^{-1}$: 3427 (br), 2852 (m), 1596 (s), 1528 (m), 1487 (m), 1463 (vs), 1441 (s), 1127 (s), 1106 (m), 1054 (m), 898 (m).

**Synthesis of [$Cu_3(\mu_3$-OH)$Cl_2(PhPyCNO)_3]\cdot 0.5H_2O$ (4)**

To a solution of Cu(II) methoxide (0.201 g, 1.6 mmol) in methanol was added phenyl 2-pyridyl ketoxime (PhPyCNOH, 0.317 g, 1.6 mmol), *tert*-butylphosphonic acid ($^tBuPO_3H_2$, 0.221 g, 1.6 mmol) and NaCl (0.021 g, 0.36 mmol). After a few days of slow evaporation compound **1** was obtained as blue prism crystals. Anal.: Found: C, 47.6; H, 3.4; N, 9.3. Calcd. for $C_{36}H_{29}Cl_2Cu_3N_6O_{4.5}$: C, 49.2; H, 3.3; N, 9.6 %. Selected IR data (KBr)/cm$^{-1}$: 3399 (br), 1596 (m), 1489 (m), 1465 (vs), 1443 (m).

**Crystallographic data collection and refinement.**

The X-Ray single-crystal data of compound **1** was collected on a Bruker X8 Kappa APEX-II diffractometer with a graphite-monochromator utilizing Mo-K$\alpha$ radiation ($\lambda$ = 0.71073 Å), with $\omega$ and $\varphi$-scans at 100(1)K.[32] Compound **2** was collected on a Bruker CCD SMART1000 diffractometer with a graphite-monochromator utilizing Mo-Kα radiation (λ = 0.71073 Å), with ω and φ-scans at 100(1)K[33] and compounds **3** and **4** were collected on a MAR345 diffractometer with an image plate detector and φ-scans at 110(2) K. The crystallographic data, conditions retained for the intensity data collection and some features of the structure refinements are listed in Table 7. Data processing, including Lorentz-polarization and absorption corrections were performed using the SADABS[34] computer programs. The structure was solved by direct methods and refined by full-matrix least-squares methods, using the SHELXTL program package.[35] All non-hydrogen atoms were refined anisotropically. The H atoms attached to C and N atoms were added theoretically and treated as riding on the concerned parent atoms. H atoms attached to O atoms were located from difference Fourier maps and included in the final refinement cycles on fixed positions.

Insert Table 7 close to here

## Conclusions

Four new trinuclear copper(II) complexes with the fragment $\{Cu_3(\mu_3\text{-OH})(\text{oximate})_3\}^{2+}$ (**1-4**) have been prepared from 2-pyridyl ketoxime derivatives and structurally characterized by X-ray crystallography. Their magnetic data have been analyzed by using an isotropic and antisymmetric exchange Hamiltonian. All these compounds show strong antiferromagnètic and antisymmetric exchange. The magnetostructural study presented here has shown a lineal correlation for complexes with the fragment $\{Cu_3(\mu_3\text{-OH})(\text{oximate})_3\}^{2+}$ between the Cu-O-Cu angle and the isotropic exchange parameters ($J$ and $j$).

## Acknowledgements

This research was supported by the Spanish Ministerio de Educación y Ciencia (MEC) (Grant CTQ2012-30662) and the Generalitat de Catalunya (Grant 2009SGR1454). We thank the Unidade de Raios X-RIAIDT, University of Santiago de Compostela, Spain, for performing intensity measurements of complexes **1** and **2.**

**Captions:**

**Figure 1.** Structure of compound **1**. Colour code: Cu(II) = light blue; N = dark blue; O = red; P = orange; Cl = green; C = grey. Hydrogen atoms have been omitted for clarity.

**Figure 2.** Dimer of trimers formed by H-bonds of compound **1**.

**Figure 3.** Structure of compound **2**. Colour code: Cu(II) = light blue; N = dark blue; O = red; P = orange; Br = purple; C = grey. Hydrogen atoms have been omitted for clarity.

**Figure 4.** Dimer of trimers formed by H-bonds of compound **2**.

**Figure 5.** Structure of compound **3**. Colour code: Cu(II) = light blue; N = dark blue; O = red; P = orange; Br = purple; C = grey. Hydrogen atoms have been omitted for clarity.

**Figure 6.** Dimer of trimers formed by H-bonds of compound **3**.

**Figure 7.** Structure of compound **4**. Colour code: Cu(II) = light blue; N = dark blue; O = red; Cl = green; C = grey. Hydrogen atoms have been omitted for clarity.

**Figure 8.** Dimer of trimers formed by H-bonds of compound **4**.

**Figure 9.** $\chi_M T$ *vs* T plot in the 300-2 K range of temperatures for complexes **1-4**. The solid lines are the best fit (see text).

**Figure 10.** Plot of the Cu-O-Cu angle *vs.* the exchange coupling constant.

**Scheme 1.**

**Scheme 2.** The angle $\beta$ is defined by the average of the most similar Cu-OH-Cu angles within the triangle, whereas the angle $\gamma$ refers to the most different one of them. The angle $\alpha$ is defined as the average of the three Cu-OH-Cu angles of the complex.

**Table 1.** Bond distances and angles of compound **1**.

**Table 2.** Bond distances and angles of compound **2**.

**Table 3.** Bond distances and angles of compound **3**.

**Table 4.** Bond distances and angles of compound **4**.

**Table 5.** Best-fit magnetic parameters for **1-4**.

**Table 6.** Magnetostructural data for **1-4**$^a$.

**Table 7.** Crystal data and structure refinement for complexes **1-4**.

## References

1 P. Chaudhuri, *Coord. Chem. Rev.*, 2003, **243**, 143.

2 C. J. Milios, C. P. Raptopoulou, A. Terzis, F. Lloret, R. Vicente, S. P. Perlepes, A. Escuer, *Angew. Chem.*, 2004, **116**, 212.

3 C. J. Milios, C. P. Raptopoulou, A. Terzis, F. Lloret, R. Vicente, S. P. Perlepes, A. Escuer, *Angew.Chem. Int. Ed.*, 2004, **43**, 210.

4 C. J. Milios, E. Kefalloniti, C. P. Raptopoulou, A. Terzis, R. Vicente, N. Lalioti, A. Escuer, S. P. Perlepes, *Chem. Commun.*, 2003, 819.

5 C. J. Milios, T. C. Stamatatos, P. Kyritsis, A. Terzis, C. P. Raptopoulou, R. Vicente, A. Escuer, S. P. Perlepes, *Eur. J. Inorg. Chem.,* 2004, 2885.

6 R. Clérac, H. Miyasaka, M. Yamashita, C. Coulon, *J. Am. Chem. Soc.*, 2002, **124**, 12837.

7 C. J. Milios, T. C. Stamatatos, S. P. Perlepes, *Polyhedron,* 2006, **25**, 134.

8 A. Chakraborty, K. L. Gurunatha, A. Muthulakshmi, S. Dutta, S. K. Pati, T. K. Maji, *Dalton Trans.*, 2012, **41**, 5879.

9 T. Afrati, C. M. Zaleski, C. Dendrinou-Samara, G. Mezel, J. W. Kampf, V. L. Pecoraro, D. P. Kessissoglou, *Dalton Trans.*, 2007, 2658.

10 M. Wenzel, R. S. Forgan, A. Faure, K. Mason, P. A. Tasker, S. Piligkos, E. K. Brechin, P. G. Plieger, *Eur. J. Inorg. Chem.,* 2009, 4613.

11 R. Beckett, B. F. Hoskins, *J. Chem. Soc., Dalton Trans.*, **1972**, 291.

12 Y.-B. Jiang, H.-Z. Kou, R.-J. Wang, A.-L. Cui, J. Ribas, *Inorg. Chem.*, 2005, **44**, 709.

13 T. Afrati, C. Dendrinou-Samara, C. Raptopoulou, A. Terzis, V. Tangoulis, D. P. Kessissoglou, *Dalton Trans.*, 2007, 5156.

14 T. Afrati, C. Dendrinou-Samara, C. Raptopoulou, A. Terzis, V. Tangoulis, D. P. Kessissoglou, *Inorg. Chem.*, 2008, **47**, 7545.

15 P. F. Ross, R. K. Murmann, E. O. Schlemper, *Acta Crystallogr., Sect. B: Struct. Crystallograph. Cryst. Chem.*, 1974, **30**, 1120.

16 G.-X. Liu, W. Guo, S. Nishihara, X.-M. Ren, *Inorg. Chim. Acta.*, 2011, **368**, 165.

17 A. Escuer, B. Cordero, M. Font-Bardia, T. Calvet, *Inorg. Chem.,* 2010, **49**, 9752.

18 R. J. Butcher, C.J. O’Connor, E. Sinn, *Inorg. Chem.,* 1981, **20**, 537.

19 Y. Agnus, R. Louis, B. Metz, C. Boudon, J. P. Gisselbrecht, M. Gross, *Inorg. Chem.*, 1991, **30**, 3155.

20 T. C. Stamatatos, J. C. Vlahopoulou, Y. Sanakis, C. P. Raptopoulou, V. Psycharis, A. K. Boudalis, S. P. Perlepes, *Inorg. Chem. Commun.,* 2006, **9**, 814.

21 T. Afrati, A.A. Pantazaki, C. Dendrinou-Samara, C. Raptopoulou, A. Terzis, D. P. Kessissoglou, *Dalton Trans.*, 2010, **39**, 765.

22 S. Ferrer, F. Lloret, E. Pardo, J.M. Clemente-Juan, M. Liu-Gonzalez and S. Garcia-Granda, *Inorg. Chem.,* 2012, **51**, 985 and references cited therein.

23 N. F. Curtis, O. P. Gladkikh, S. L. Heath and K. R. Morgan, *Aust. J. Chem.*, 2000, **53**, 577.

24 P. Chakrabarti, V. G. Puranik, J. P. Naskar, S. Hati and D. Datta, *Indian J. Chem.*, 2000, **39A**, 571.

25 S. Ferrer, E. Aznar, F. Lloret, A. Castiñeiras, M. Liu-González and J. Borrás, *Inorg. Chem.,* 2007, **46**, 372.

26 M. Wenzel, R. S. Forgan, A. Faure, K. Mason, P. A. Tasker, S. Piligkos, E. K. Brechin and P. G. Plieger, *Eur. J. Inorg. Chem.*, 2009, 4613.

27 D. Maity, P. Mukherjee, A. Ghosh, M. G. B. Drew, C. Diaz and G. Mukhopadhyay, *Eur. J. Inorg. Chem.*, 2010, 807.

28 S. Karmakar, O. Das, S. Ghosh, E. Zangrando, M. Johann, E. Rentschler, T. Weyhermüller, S. Khanra and T. K. Paine, *Dalton Trans.*, 2010, **39**, 10920.

29 V. Chandrasekhar, T. Senapati, A. Dey, S. Hossain, *Dalton Trans.,* 2011, **40**, 5394.

30 E. S. Koumousi, C. P. Raptopuolou, S. P. Perlepes. A. Escuer, T. C. Stamatatos, *Polyhedron,* 2010, **29**, 204 and references therein.

31 A. W. Addison, T. N. Rao, J. Reedijk, J. V. Rijjin, G. C. Verschoor, *J. Chem. Soc., Dalton Trans.,* 1984, 1349.

32 Bruker Analytical X-ray Systems, APEX2: Bruker AXS Inc., Version 2009-3.0, 2009.

33 Bruker Analytical X-ray Systems, SMART: Bruker Molecular Analysis Research Tool, Version 5.054, 1997-98.

34 G. M. Sheldrick, SADABS, v. 2, University of Göttingen, Germany, 2001.

35 G. M. Sheldrick, *Acta Crystallogr.*, 2008, **A64**, 112.

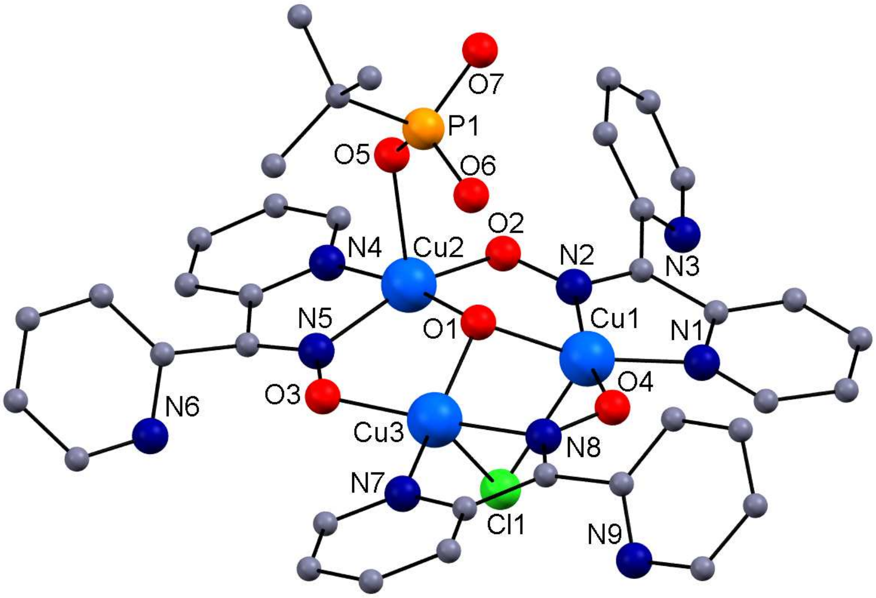

**Figure 1**

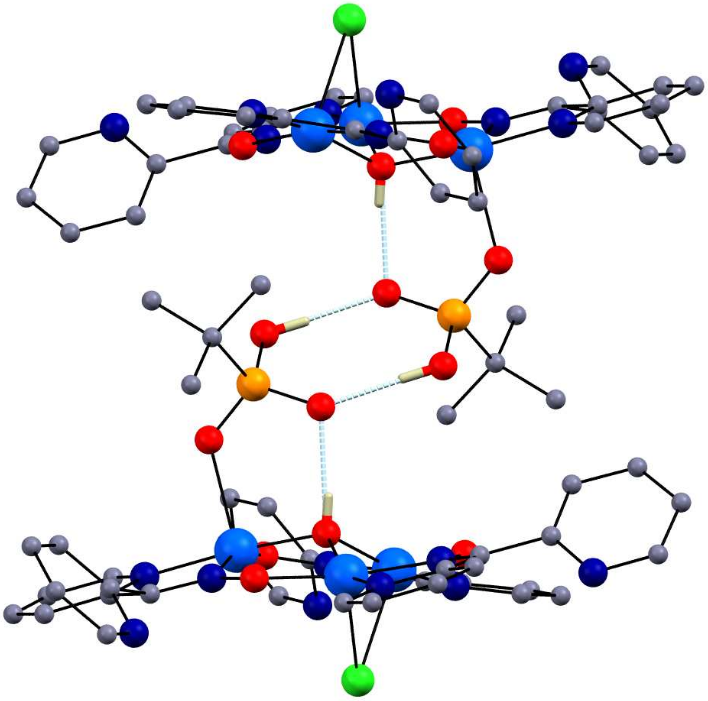

**Figure 2**

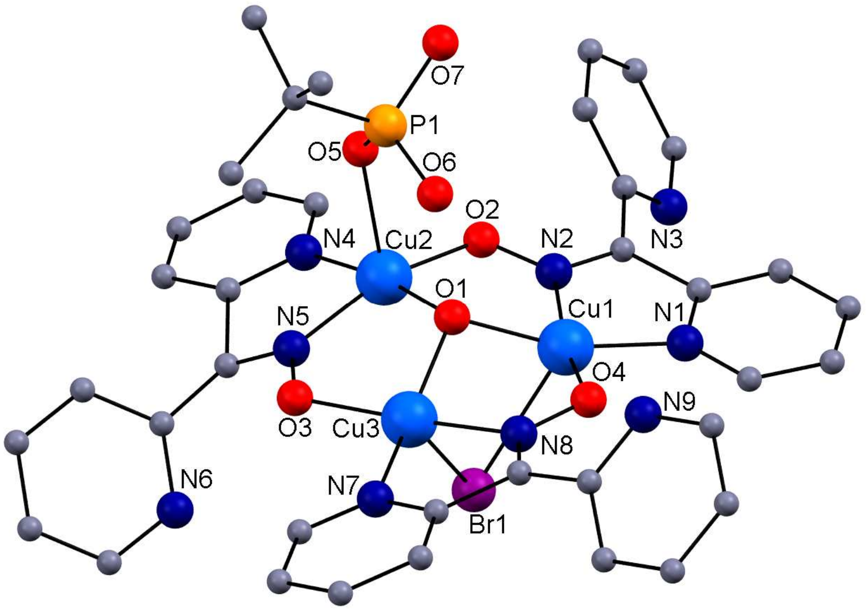

Figure 3

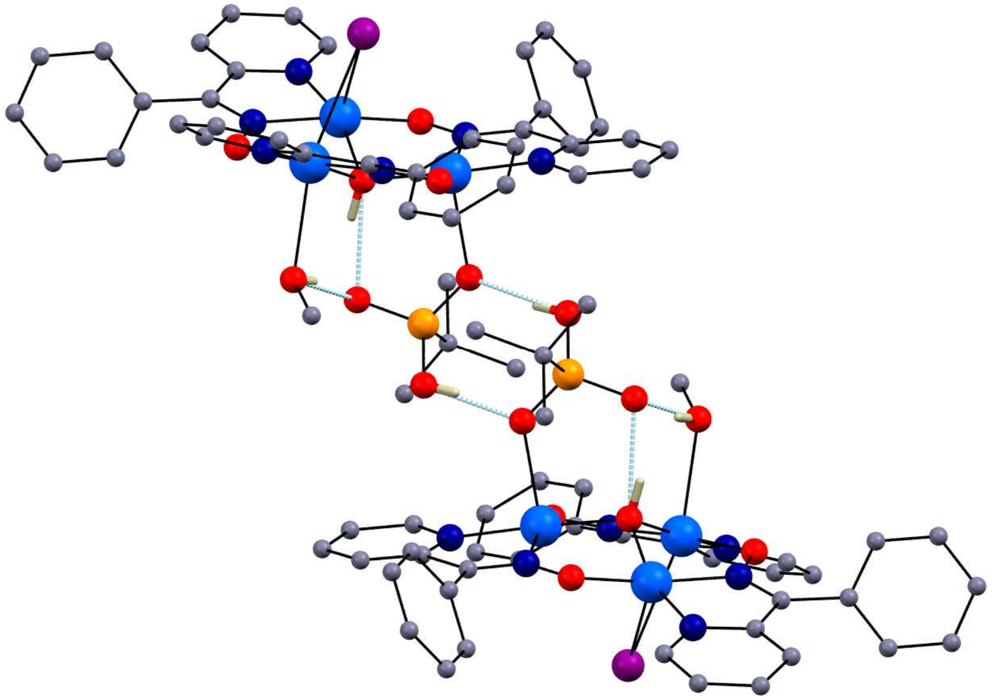

Figure 4

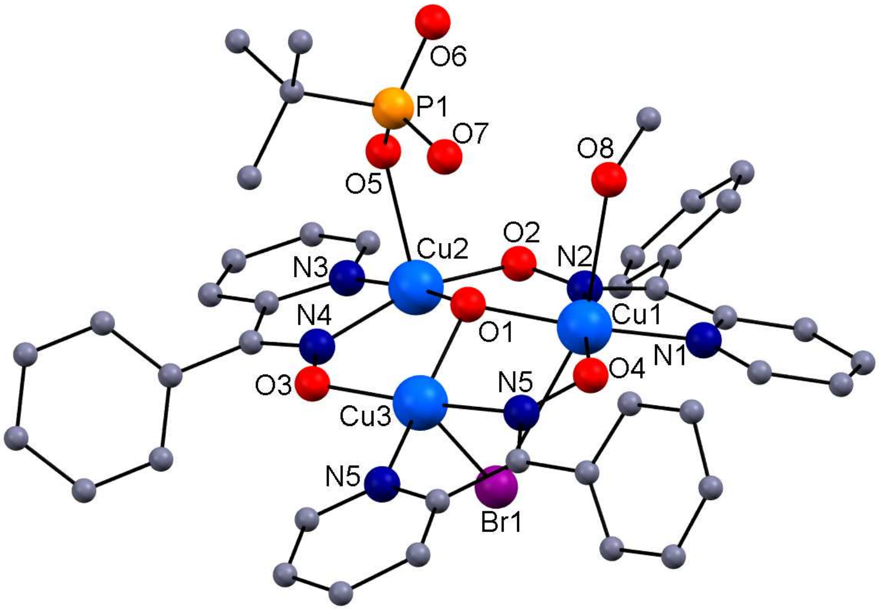

**Figure 5**

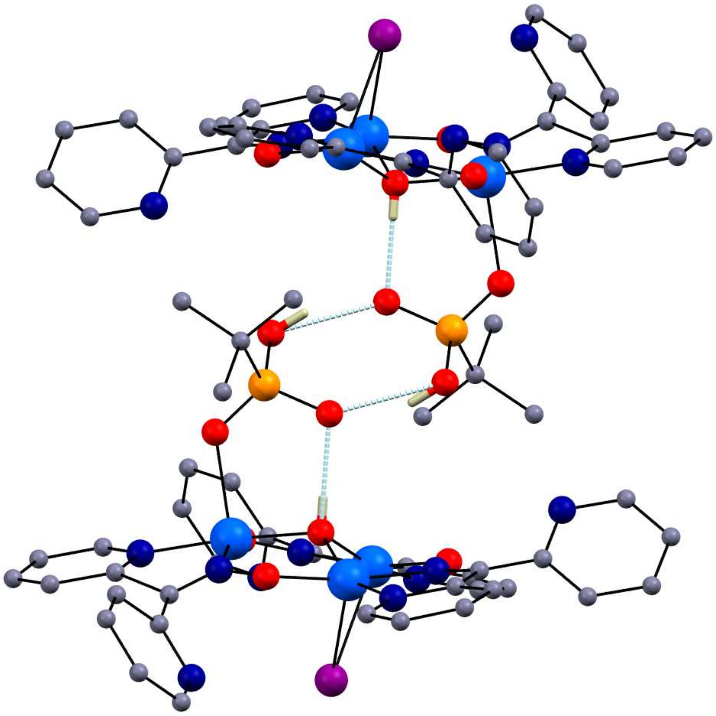

**Figure 6**

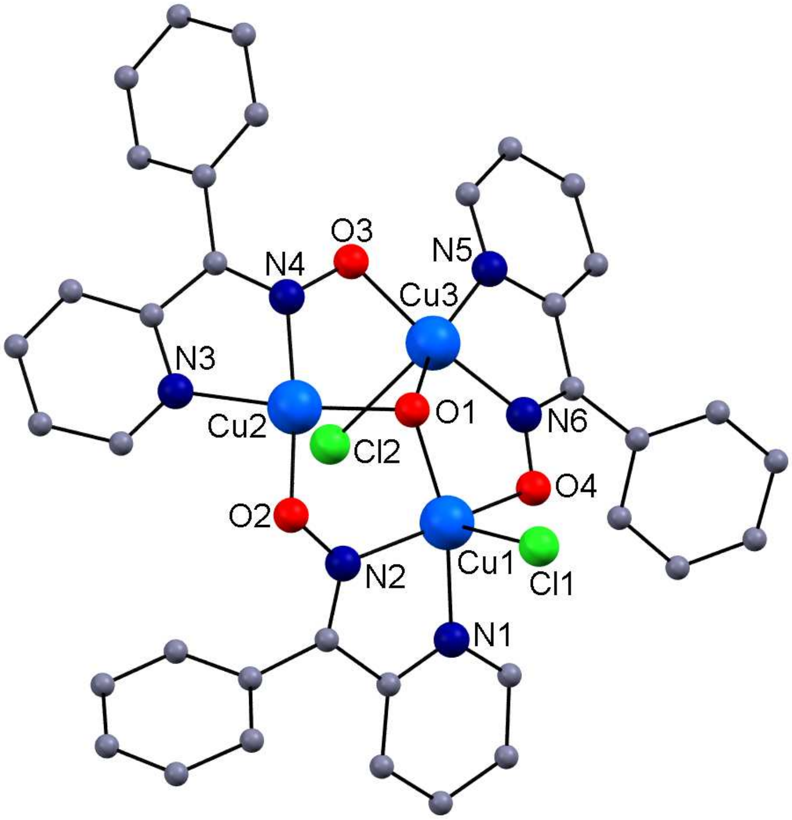

Figure 7

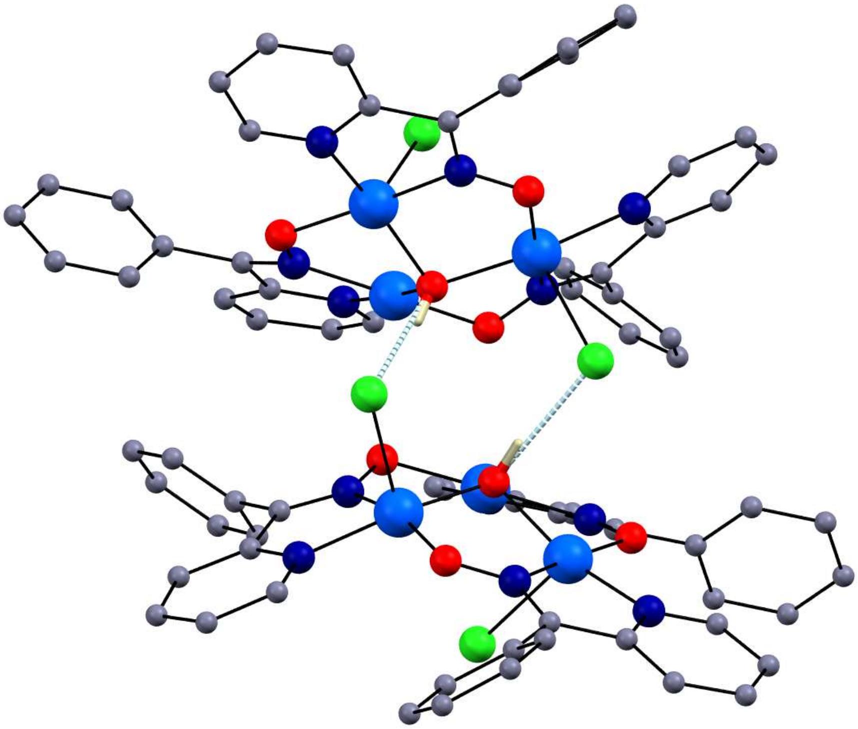

Figure 8

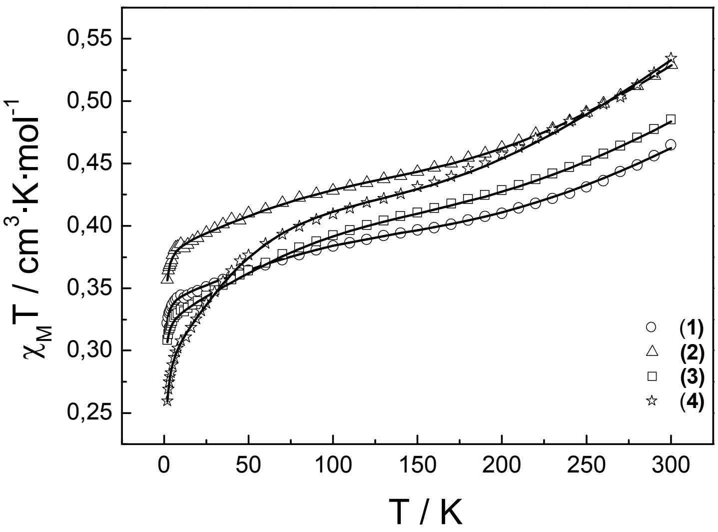

**Figure 9**

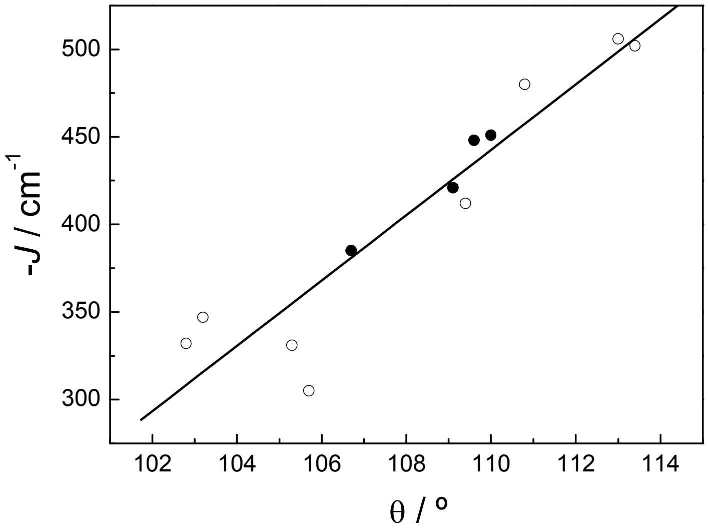

**Figure 10**

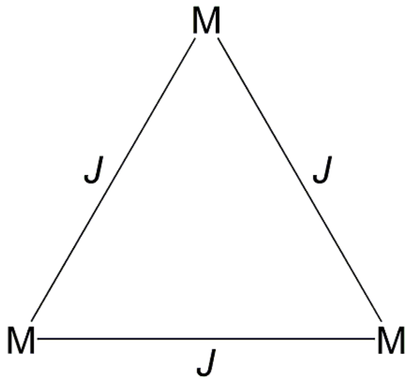

Scheme 1

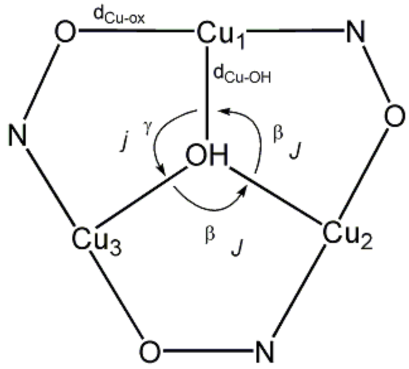

Scheme 2

**Table 1**

| | | | | | | | |
|---|---|---|---|---|---|---|---|
| Bond distances (Å) | | | | | | | |
| Cu1-Cl1 | 2.633(6) | Cu1-O1 | 1.947(4) | Cu1-O2 | 2.928(3) | Cu1-O4 | 1.947(3) |
| Cu1-N1 | 1.974(4) | Cu1-N2 | 1.976(4) | Cu2-O1 | 1.931(3) | Cu2-O2 | 1.945(4) |
| Cu2-O3 | 2.927(4) | Cu2-O5 | 2.293(4) | Cu2-N4 | 1.950(3) | Cu2-N5 | 1.983(5) |
| Cu3-Cl1 | 2.684(5) | Cu3-O1 | 1.947(4) | Cu3-O3 | 1.920(4) | Cu3-O4 | 2.896(3) |
| Cu3-N7 | 1.963(4) | Cu3-N8 | 1.963(4) | | | | |
| Bond angles (º) | | | | | | | |
| Cl1-Cu1-O1 | 80.97(16) | Cl1-Cu1-O2 | 92.19(13) | Cl1-Cu1-O4 | 91.63(16) | Cl1-Cu1-N1 | 112.63(17) |
| Cl1-Cu1-N2 | 101.32(16) | O1-Cu1-O2 | 66.75(13) | O1-Cu1-O4 | 92.60(15) | O1-Cu1-N1 | 164.15(17) |
| O1-Cu1-N2 | 88.09(16) | O2-Cu1-O4 | 158.09(14) | O2-Cu1-N1 | 103.38(15) | O4-Cu1-N1 | 95.00(17) |
| O4-Cu1-N2 | 166.97(15) | N1-Cu1-N2 | 81.40(16) | O1-Cu2-O2 | 92.69(15) | O1-Cu2-O3 | 67.32(13) |
| O1-Cu2-O5 | 94.04(14) | O1-Cu2-N4 | 170.45(17) | O1-Cu2-N5 | 89.62(18) | O2-Cu2-O3 | 152.52(15) |
| O2-Cu2-O5 | 94.02(15) | O2-Cu2-N4 | 94.84(15) | O2-Cu2-N5 | 160.48(19) | O3-Cu2-O5 | 105.59(14) |
| O3-Cu2-N4 | 103.60(13) | O5-Cu2-N4 | 91.30(14) | O5-Cu2-N5 | 105.16(18) | N4-Cu2-N5 | 81.33(18) |
| Cl1-Cu3-O1 | 79.64(18) | Cl1-Cu3-O3 | 103.94(17) | Cl1-Cu3-O4 | 72.89(12) | Cl1-Cu3-N7 | 117.54(18) |
| Cl1-Cu3-N8 | 85.91(16) | O1-Cu3-O3 | 93.53(16) | O1-Cu3-O4 | 67.86(12) | O1-Cu3-N7 | 158.84(14) |
| O1-Cu3-N8 | 88.74(15) | O3-Cu3-O4 | 161.37(15) | O3-Cu3-N7 | 93.90(16) | O3-Cu3-N8 | 170.13(19) |
| O4-Cu3-N7 | 103.87(12) | N7-Cu3-N8 | 80.80(15) | Cu1-O1-Cu3 | 102.76(18) | Cu2-O1-Cu3 | 112.77(17) |
| Cu1-O1-Cu2 | 113.32(19) | | | | | | |

**Table 2**

| | | | | | | | |
|---|---|---|---|---|---|---|---|
| Bond distances (Å) | | | | | | | |
| Br1-Cu1 | 2.855(1) | Br1-Cu3 | 2.740(1) | Cu1-O1 | 1.939(3) | Cu1-O2 | 2.927(3) |
| Cu1-O4 | 1.938(3) | Cu1-N1 | 1.977(4) | Cu1-N2 | 1.970(4) | Cu2-O1 | 1.928(3) |
| Cu2-O2 | 1.949(4) | Cu2-O3 | 2.932(4) | Cu2-O5 | 2.276(4) | Cu2-N4 | 1.946(3) |
| Cu2-N5 | 1.956(5) | Cu3-O1 | 1.944(3) | Cu3-O3 | 1.935(3) | Cu3-O4 | 2.888(3) |
| Cu3-N7 | 1.982(4) | Cu3-N8 | 1.967(3) | | | | |
| Bond angles (º) | | | | | | | |
| Cu1-Br1-Cu3 | 65.84(2) | Br1-Cu1-O1 | 79.24(8) | Br1-Cu1-O2 | 90.50(7) | Br1-Cu1-O4 | 92.84(9) |
| Br1-Cu1-N1 | 115.06(11) | Br1-Cu1-N2 | 100.28(10) | O1-Cu1-O2 | 67.06(10) | O1-Cu1-O4 | 92.46(12) |
| O1-Cu1-N1 | 163.53(14) | O1-Cu1-N2 | 88.25(14) | O2-Cu1-O4 | 158.24(10) | O2-Cu1-N1 | 103.22(12) |
| O4-Cu1-N1 | 94.80(13) | O4-Cu1-N2 | 166.76(13) | N1-Cu1-N2 | 81.34(15) | O1-Cu2-O2 | 92.97(12) |
| O1-Cu2-O3 | 67.33(10) | O1-Cu2-O5 | 93.83(11) | O1-Cu2-N4 | 170.98(17) | O1-Cu2-N5 | 89.75(16) |
| O2-Cu2-O3 | 152.94(12) | O2-Cu2-O5 | 94.17(14) | O2-Cu2-N4 | 94.42(16) | O2-Cu2-N5 | 160.26(18) |
| O3-Cu2-O5 | 105.09(13) | O3-Cu2-N4 | 103.98(16) | O5-Cu2-N4 | 90.80(15) | O5-Cu2-N5 | 105.16(18) |
| N4-Cu2-N5 | 81.6(2) | Br1-Cu3-O1 | 82.20(8) | Br1-Cu3-O3 | 100.43(11) | Br1-Cu3-O4 | 77.60(6) |
| Br1-Cu3-N7 | 116.24(12) | Br1-Cu3-N8 | 90.07(11) | O1-Cu3-O3 | 93.28(14) | O1-Cu3-O4 | 67.56(10) |
| O1-Cu3-N7 | 158.49(15) | O1-Cu3-N8 | 88.75(14) | O3-Cu3-O4 | 160.83(14) | O3-Cu3-N7 | 93.97(17) |
| O3 -Cu3-N8 | 169.49(16) | O4-Cu3-N7 | 104.05(14) | N7-Cu3-N8 | 80.67(17) | Cu1-O1-Cu2 | 113.45(13) |
| Cu1-O1-Cu3 | 103.18(13) | Cu2-O1-Cu3 | 113.19(13) | | | | |

**Table 3**

| | | | | | | | |
|---|---|---|---|---|---|---|---|
| Bond distances (Å) | | | | | | | |
| Br1-Cu1 | 3.123(1) | Br1-Cu3 | 2.726(1) | Cu1-O1 | 1.933(2) | Cu1-O2 | 2.917(3) |
| Cu1-O4 | 1.947(3) | Cu1-O8 | 2.537(5) | Cu1-N1 | 1.977(3) | Cu1-N2 | 1.975(3) |
| Cu2-O1 | 1.948(2) | Cu2-O2 | 1.956(3) | Cu2-O3 | 2.932(3) | Cu2-O5 | 2.316(3) |
| Cu2-N3 | 1.970(3) | Cu2-N4 | 1.977(3) | Cu3-O1 | 1.967(3) | Cu3-O3 | 1.933(3) |
| Cu3-O4 | 2.903(3) | Cu3-N5 | 1.981(3) | Cu3-N6 | 1.974(3) | | |
| Bond angles (º) | | | | | | | |

| | | | | | | | |
|---|---|---|---|---|---|---|---|
| Cu1-Br1-Cu3 | 63.67(3) | Br1-Cu1-O1 | 74.80(9) | Br1-Cu1-O2 | 81.35(6) | Br1-Cu1-O4 | 89.06(9) |
| Br1-Cu1-O8 | 161.43(10) | Br1-Cu1-N1 | 107.55(11) | Br1-Cu1-N2 | 87.75(9) | O1-Cu1-O2 | 69.46(9) |
| O1-Cu1-O4 | 92.80(10) | O1-Cu1-O8 | 86.98(13) | O1-Cu1-N1 | 172.66(11) | O1-Cu1-N2 | 91.34(11) |
| O2-Cu1-O4 | 161.49(9) | O2-Cu1-O8 | 89.06(11) | O2-Cu1-N1 | 103.77(10) | O4-Cu1-O8 | 95.45(13) |
| O4-Cu1-N1 | 94.19(11) | O4-Cu1-N2 | 173.93(13) | O8-Cu1-N1 | 90.12(14) | O8-Cu1-N2 | 89.20(13) |
| N1-Cu1-N2 | 81.87(12) | O1-Cu2-O2 | 94.99(10) | O1-Cu2-O3 | 67.63(9) | O1-Cu2-O5 | 93.01(11) |
| O1-Cu2-N3 | 170.53(11) | O1-Cu2-N4 | 89.64(12) | O2-Cu2-O3 | 153.48(10) | O2-Cu2-O5 | 96.07(12) |
| O2-Cu2-N3 | 94.30(11) | O2-Cu2-N4 | 160.95(14) | O3-Cu2-O5 | 104.41(9) | O3-Cu2-N3 | 103.01(10) |
| O5-Cu2-N3 | 87.86(13) | O5-Cu2-N4 | 102.15(12) | N3-Cu2-N4 | 80.96(12) | Br1-Cu3-O1 | 84.77(8) |
| Br1-Cu3-O3 | 101.57(8) | Br1-Cu3-O4 | 80.86(6) | Br1-Cu3-N5 | 108.03(10) | Br1-Cu3-N6 | 89.37(9) |
| O1-Cu3-O3 | 93.30(10) | O1-Cu3-O4 | 67.32(9) | O1-Cu3-N5 | 162.89(13) | O1-Cu3-N6 | 88.64(11) |
| O3-Cu3-O4 | 160.32(10) | O3-Cu3-N5 | 95.09(12) | O3-Cu3-N6 | 169.02(12) | O4-Cu3-N5 | 102.77(11) |
| N5-Cu3-N6 | 80.40(13) | Cu1-O1-Cu2 | 112.01(11) | Cu1-O1-Cu3 | 105.47(12) | Cu2-O1-Cu3 | 109.13(12) |

**Table 4**

| | | | | | | | |
|---|---|---|---|---|---|---|---|
| Bond distances (Å) | | | | | | | |
| Cu1-Cl1 | 2.508(2) | Cu1-O1 | 1.986(2) | Cu1-O2 | 2.929(3) | Cu1-O4 | 1.948(3) |
| Cu1-N1 | 2.012(3) | Cu1-N2 | 1.993(3) | Cu2-Cl2 | 3.019(2) | Cu2-O1 | 1.944(2) |
| Cu2-O2 | 1.935(3) | Cu2-O3 | 2.910(3) | Cu2-N3 | 1.978(3) | Cu2-N4 | 1.973(3) |
| Cu3-Cl2 | 2.600(2) | Cu3-O1 | 1.989(3) | Cu3-O3 | 1.951(3) | Cu3-O4 | 2.899(3) |
| Cu3-N5 | 1.995(4) | Cu3-N6 | 1.971(3) | | | | |
| Bond angles (º) | | | | | | | |
| Cl1-Cu1-O1 | 98.52(8) | Cl1-Cu1-O2 | 98.91(7) | Cl1-Cu1-O4 | 95.37(9) | Cl1-Cu1-N1 | 93.53(11) |
| Cl1-Cu1-N2 | 99.23(10) | O1-Cu1-O2 | 66.65(9) | O1-Cu1-O4 | 94.30(11) | O1-Cu1-N1 | 164.80(12) |
| O1-Cu1-N2 | 88.95(11) | O2-Cu1-O4 | 157.62(10) | O2-Cu1-N1 | 102.44(11) | O4-Cu1-N1 | 93.75(12) |
| O4-Cu1-N2 | 164.40(13) | N1-Cu1-N2 | 79.96(13) | Cl2-Cu2-O1 | 72.50(8) | Cl2-Cu2-O2 | 101.69(9) |
| Cl2-Cu2-O3 | 69.52(6) | Cl2-Cu2-N3 | 106.40(11) | Cl2-Cu2-N4 | 79.58(10) | O1-Cu2-O2 | 92.99(10) |
| O1-Cu2-O3 | 69.52(9) | O1-Cu2-N3 | 173.26(13) | O1-Cu2-N4 | 92.45(12) | O2-Cu2-O3 | 161.95(8) |
| O2-Cu2-N3 | 93.75(12) | O2-Cu2-N4 | 174.55(12) | O3-Cu2-N3 | 103.79(11) | N3-Cu2-N4 | 80.82(14) |
| Cl2-Cu3-O1 | 82.47(8) | Cl2-Cu3-O3 | 94.91(8) | Cl2-Cu3-O4 | 80.87(6) | Cl2-Cu3-N5 | 115.53(10) |
| Cl2-Cu3-N6 | 90.17(9) | O1-Cu3-O3 | 93.88(11) | O1-Cu3-O4 | 69.49(9) | O1-Cu3-N5 | 160.04(12) |
| O1-Cu3-N6 | 90.96(12) | O3-Cu3-O4 | 163.19(10) | O3-Cu3-N5 | 93.07(12) | O3-Cu3-N6 | 173.40(12) |
| O4-Cu3-N5 | 103.46(11) | N5-Cu3-N6 | 80.91(13) | Cu1-O1-Cu2 | 109.38(11) | Cu1-O1-Cu3 | 106.68(11) |
| Cu2-O1-Cu3 | 104.32(12) | | | | | | |

**Table 5**

| Complex | $-J_{av}$ | $\theta$ | $\delta$ | $G$ | $g_{\|\|}$ | $g_{\perp}$ |
|---|---|---|---|---|---|---|
| **1** | 448 | -0.12 | 176 | 62 | 2.26 | 2.01 |
| **2** | 451 | -0.14 | 158 | 73 | 2.29 | 2.10 |
| **3** | 422 | -0.16 | 176 | 62 | 2.35 | 2.06 |
| **4** | 385 | -0.34 | 82 | 47 | 2.22 | 2.13 |

**Table 6**

| Complex | $-J_{av}$ | α | $-J$ | β | $-j$ | γ | $d_{Cu-ox}$ | $d_{Cu-OH}$ |
|---|---|---|---|---|---|---|---|---|
| **1** | 448 | 109.7 | 507 | 113.1 | 331 | 102.8 | 1.956 | 1.941 |
| **2** | 451 | 110.0 | 503 | 113.4 | 345 | 103.4 | 1.952 | 1.935 |
| **3** | 422 | 109.0 | 480 | 110.7 | 304 | 105.6 | 1.961 | 1.948 |
| **4** | 385 | 106.8 | 331 | 105.5 | 413 | 109.4 | 1.962 | 1.973 |

[a]The parameters are defined in Scheme 2. The distances and bond angles are average values.

**Table 7**

| | **1** | **2** | **3** | **4** |
|---|---|---|---|---|
| formula | $C_{37}H_{43}ClCu_3N_9O_{11}P$ | $C_{74}H_{84}Br_2Cu_6N_{18}O_{21}P_2$ | $C_{170}H_{192}Br_4Cu_{12}N_{24}O_{38}P_4$ | $C_{144}H_{116}Cl_8Cu_{12}N_{24}O_{18}$ |
| weight | 1046.84 | 2164.59 | 4385.48 | 3516.69 |
| crystal system | triclinic | triclinic | monoclinic | monoclinic |
| space group | P-1 | P-1 | C2/c | C2/c |
| a (Å) | 12.4303(4) | 12.302(3) | 34.556(13) | 28.805(11) |
| b (Å) | 13.4622(5) | 13.355(3) | 12.953(5) | 10.739(4) |
| c (Å) | 15.7280(8) | 15.779(5) | 23.542(4) | 27.103(6) |
| α (°) | 106.861(3) | 109.133(4) | 90 | 90 |
| β (°) | 96.972(3) | 95.518(4) | 104.03(2) | 109.63(2) |
| γ (°) | 113.633(2) | 113.774(3) | 90 | 90 |
| V ($Å^3$) | 2184.0(2) | 2161.8(1) | 10223(6) | 7897(5) |
| Z | 2 | 1 | 2 | 2 |
| $\rho_{calc}$ (g $cm^{-3}$) | 1.592 | 1.663 | 1.425 | 1.479 |
| F(000) | 1070 | 1096 | 4464 | 3552 |
| mu($mm^{-1}$) | 1.613 | 2.490 | 2.105 | 1.782 |
| T (K) | 100.0(1) | 100.0(1) | 293(2) | 293(2) |
| $R^a$ [$I > 2\sigma(I)$] | 0.0489 | 0.0418 | 0.0573 | 0.0577 |
| $wR^b$ [$I > 2\sigma(I)$] | 0.1108 | 0.1014 | 0.1652 | 0.1495 |
| $S^c$ | 1.047 | 1.002 | 1.067 | 1.072 |

[a]R $= \sum\left(|F_0| - |F_c|\right)/\sum|F_0|$. [b]ωR $= \left[\sum w\left(|F_0| - |F_c|\right)^2 / \sum w|F_0|^2\right]^{1/2}$. [c]Σ $= \left[\sum w\left(|F_0| - |F_c|^2\right)/\left(N_0 - N_p\right)\right]^{1/2}$